

STATISTICAL SIMILARITY MEASURE FOR OIL SLICK DETECTION IN SAR IMAGE

Bahia Lounis[‡], Grégoire Mercier[†] and Aichouche Belhadj-Aissa[‡]

[‡] Université des Sciences & Technologie
Houari Boumediene (USTHB),
BP32 El Alia, Bab Ezzouar
Fac. d'Electronique & Informatique / LTIR
16111, Alger, Algeria.

[†] Institut Telecom; Telecom Bretagne
CNRS FRE 3167 lab-STICC, team CID
Technopole Brest-Iroise,
CS 83818, F-29238 Brest Cedex 3, France

ABSTRACT

Spaceborne Synthetic Aperture Radar (SAR) is well adapted to detect ocean pollution independently from daily or weather condition. As it is sensitive to surface roughness, the presence of oil film on the sea surface decreases the backscattering of the sea surface resulting in a dark feature patches in SAR images. In fact, oil slicks have specific impact on ocean wave spectra. Initial wave spectra may be characterized by three kinds of waves, big, medium and small, which correspond physically to gravity and gravity-capillary waves. The increase of viscosity due to the presence of oil damps gravity-capillary waves. This induces a damping of the backscattering to the sensor, but also a damping of the energy of the wave spectra, then it modifies the sea surface roughness observed by the sensor. Thus, local detection of wave spectra modification may be achieved by a appropriated texture analysis of the original SAR image.

In this paper, the texture analysis is based on measure of similarity between a local probability density function (pdf) of clean water and the local pdf of the zone to be inspected. The local distribution is estimated in the neighbourhood of each pixel, through a sliding window, and compared to the reference one by using the Kullback-Leibler (KL) distance between distributions. An efficient strategy has been adopted in order to perform pdf estimation through a non-parametric approach. The reference area, given by an expert, allows the texture analysis to better discriminate oil slick areas from low-wind or low-wave areas of clean water.

The algorithm has been applied on Envisat ASAR images. It yields accurate segmentation results, even for small slicks, with a limited number of false alarms.

1. INTRODUCTION

Oil spills cause substantial damage to the marine environment and demands consequently for necessary prevention policy. In this field, Synthetic Aperture Radar (SAR) images are widely used to detect and monitor oil pollution on the sea surface since they provide regularly images both day and

night and are insensitive to meteorological effects. As it is sensitive to surface roughness, the presence of oil film on the sea surface decreases the backscattering of the sea surface resulting in a dark feature patches in SAR images [1].

Automatic analysis of SAR images is not applied routinely yet. After the SAR data acquisition, a quick inspection of the imaged areas is performed. Only images with features suspected to be oil slicks are processed in full resolution mode: Precision Image format (PRI) for ERS and ENVISAT data and PathImage for Radarsat data. Then, the detection and identification procedure is started. The procedure is operated in either manual or automatic mode. For manual operation, an operator inspects the scene, selects portions of the image that might contain slicks, and applies segmentation algorithms in order to extract oil signatures. In automatic mode, the system selects the areas of low backscatter and then segments the image. At the end of both processes a detection report is generated in order to aid clean up operations, provide damage assessment and help polluters identification [1].

In this paper, a new method in a semi-supervised mode is presented which consists in SAR image inspection in order to highlight the spots suspected to be oil slicks (mostly dark spot but also affecting by sea-surface wave spectrum damping that induces a shade of texture). The method is based on measure of similarity between a local probability density function (pdf) of clean water and the local pdf of the zone to be inspected. The local distribution is estimated in the neighbourhood of each pixel, through a sliding window, and compared to the reference one by using the Kullback-Leibler (KL) distance between distributions [2].

The KL distance is computed in a local window of increasing size. Smaller window size is appropriated to small slick detection but with the drawback of mixing up with many false alarms. On the contrary, larger window size ensure the detection but with the drawback to miss-detect smaller slicks and smooth the border of the slicks. Furthermore, it is proposed to adjust the form of analysis window in order to select a local homogeneous area when a transition occurs.

In this context, edges are detected through a multiscale gradient operator that prevent from noisy gradient direction estimation since sea-surface remains highly textured on SAR images. This multiscale gradient operator takes also the advantage of the multiscale analysis of sea-surface wave spectra which is able to characterize the modifications of the wave direction and amplitude induced by the presence of a film on the sea surface [3].

2. SIMILARITY MEASURE

Slick detection is perform by a comparison of the pdf, estimated within a sliding window, and a pdf defined by an expert over a region of interest (ROI) characterizing a *normal* sea state.

2.1. Local pdf estimation

Let consider a set of n samples $\{x_1, x_2, \dots, x_n\}$ taken from a sliding window or a ROI. It characterizes the sampling of a random variable (RV) X . The pdf of X is estimated through a non parametric approach by using a cumulant-based approximation. The cumulants themselves do not provide such a pdf estimation directly but are necessary to *describe* its shape: for example, third order (κ_3) is linked to the symmetry (*i.e.* skewness), while the fourth (κ_4) to the flatness (*i.e.* kurtosis). The density is then estimated through a series expansion. Actually, the cumulant generating function is used for such an estimation. By definition, the cumulant generating function $\mathcal{K}_X(\cdot)$ of a random variable X is defined by:

$$\mathcal{K}_X(\omega) = \ln \mathcal{M}_X(\omega) = \sum_n \kappa_{X;n} \frac{\omega^n}{n!}$$

with $\mathcal{M}_X(\cdot)$ being the moment generating function:

$$\begin{aligned} \mathcal{M}_X(\omega) &= \int e^{\omega x} f_X(x) dx \\ &= \int \left(1 + \omega x + \frac{\omega^2}{2} x^2 + \dots\right) f_X(x) dx. \end{aligned}$$

For the case of the four first order cumulants, the following expressions hold [4, p.8]:

$$\begin{aligned} \kappa_{X;1} &= \mu_{X;1} \\ \kappa_{X;2} &= \mu_{X;2} - \mu_{X;1}^2 \\ \kappa_{X;3} &= \mu_{X;3} - 3\mu_{X;2}\mu_{X;1} + 2\mu_{X;1}^3 \\ \kappa_{X;4} &= \mu_{X;4} - 4\mu_{X;3}\mu_{X;1} - 3\mu_{X;2}^2 + 12\mu_{X;2}\mu_{X;1}^2 - 6\mu_{X;1}^4. \end{aligned} \quad (1)$$

Let us assume that the density to be approximated is not *too far* from a Gaussian pdf (denoted as \mathcal{G}_X to underline the fact that it has the same mean and variance as X). The difference between $\mathcal{K}_X(\cdot)$ and $\mathcal{K}_{\mathcal{G}_X}(\cdot)$, gives a link between $\mathcal{K}_X(\omega)$ and $\mathcal{K}_{\mathcal{G}_X}(\cdot)$ through the difference of the cumulants $\kappa_{X;n} -$

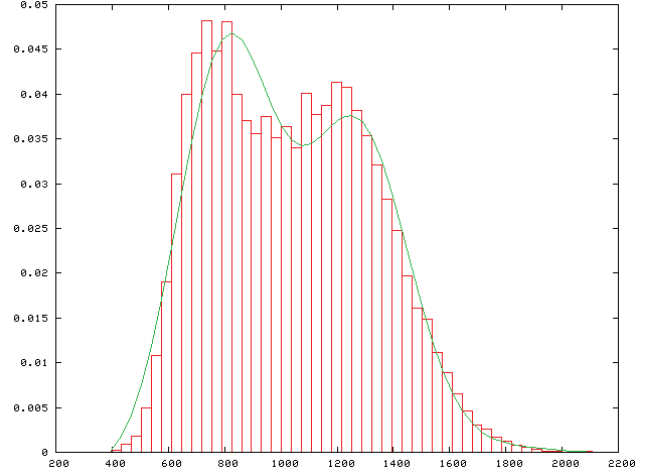


Fig. 1. Estimation of an histogram from a cumulant-based expansion.

$\kappa_{\mathcal{G}_X;n}$. By inversion, the density may be expressed by a formal Taylor-like series:

$$f_X(x) = \mathcal{G}_X(x) + c_1 \frac{d\mathcal{G}_X}{dx} + c_2 \frac{d^2\mathcal{G}_X}{dx^2} + \dots$$

Since a Gaussian density is used, it comes

$$f_X(x) = \sum_{r=0}^{\infty} c_r H_r(x) \mathcal{G}_X(x),$$

with $H_r(x)$ known as the Chebyshev-Hermite polynomial of order r [5]. When choosing a Gaussian law so that its first and second cumulants agree with those of X , the number of terms of the series expansion is greatly reduced. This is the so-called Edgeworth series expansion. Its expression, when truncated to order 6, is the following:

$$\begin{aligned} f_X(x) &= \left(1 + \frac{\kappa_{X';3}}{6} H_3(x) + \frac{\kappa_{X';4}}{24} H_4(x) + \frac{\kappa_{X';5}}{120} H_5(x) \right. \\ &\quad \left. + \frac{\kappa_{X';6} + 10\kappa_{X';3}^2}{720} H_6(x)\right) \mathcal{G}_X(x). \end{aligned} \quad (2)$$

It can be thought of as a model of the form $X = X_G + X'$ where X_G is a random variable with Gaussian density with same mean and variance as X , and X' (a standardized version of X with $X' = (X - \kappa_{X;1})\kappa_{X;2}^{-1/2}$ [6]). Fig 1 shows an example of such an approximation of a histogram taken from an Envisat ASAR image, in a heterogeneous area where an oil slick is mixed up to clean water.

2.2. Efficient comparison

The Edgeworth series expansion of the two pdfs f_X and f_Y may be introduced into the Kullback-Leibler divergence, de-

defined as:

$$K(Y|X) = \int \log f_X(x) \frac{f_X(x)}{f_Y(x)} f_X(x) dx. \quad (3)$$

It yields an approximation of the Kullback-Leibler divergence by Edgeworth series, truncated at a given order. In [7], such an approximation has been given up to order 4 by using the equality $\frac{f_X}{f_Y} = \frac{f_X}{\mathcal{G}_X} \frac{\mathcal{G}_X}{\mathcal{G}_Y} \frac{\mathcal{G}_Y}{f_Y}$, where \mathcal{G}_X (resp. \mathcal{G}_Y) is a Gaussian density of same mean and variance as f_X (resp. f_Y). It comes a similarity measure between two pdfs, depending on cumulants of X and Y for which the full description is given in eq. (11) of [2]. It has been turned to be symmetrical by using:

$$K_{\text{Edgeworth}}(X|Y) + K_{\text{Edgeworth}}(Y|X). \quad (4)$$

2.3. Sample selection

As show on fig. 1, pdf estimation in mixture oil-no oil area may not be representative to local characteristic of the sea surface. Hence, it is necessary to select the appropriated neighbourhood of the central pixel in a sliding window. Sample selection may be investigated in two ways. Each of them requires the use of external data.

1. The first strategy consists in using structural information issued from a gradient measure. In fact, normal gradient remains too sensitive to the noise induced by surface roughness and the presence of the waves. Gradient measure comes from a multiscale differential operator issued from a wavelet-based multiscale operator [3].

The decomposition of an image I (where the pixel value at position (x, y) is denoted $I(x, y)$) is achieved by a convolution with a smoothing function $\theta(x, y) = \theta(x)\theta(y)$ that yields the smoothed image denoted by I_1^{low} . Two convolutions with the wavelets $\psi^x(x)$ and $\psi^y(y)$ are also applied on images I to yield *gradient* images at scale $\ell = 1$, denoted by $W_1^x I(x, y) = I *^x \psi^x(x) = \frac{d}{dx} (I *^x \theta(x))$ and $W_1^y I(x, y) = I *^y \psi^y(y) = \frac{d}{dy} (I *^y \theta(y))$. $*^x$ (resp. $*^y$) stands for the convolution on x (resp. y) only. At coarser level, the decomposition is applied on the smoothed image I_ℓ^{low} so that the overall decomposition up to a scale L may be denote as the set of $2L + 1$ images:

$$I \longrightarrow \begin{cases} I_L^{\text{low}} & = I * \theta \left(\frac{x}{2^{(L-1)}}, \frac{y}{2^{(L-1)}} \right) \\ W_\ell^x I & = \frac{d}{dx} \left(I *^x \theta \left(\frac{x}{2^\ell} \right) \right) \\ W_\ell^y I & = \frac{d}{dy} \left(I *^y \theta \left(\frac{y}{2^\ell} \right) \right) \end{cases} \quad (5)$$

with $0 \leq \ell < L$.

The modulus of $(W_{\ell=4}^x I, W_{\ell=4}^y I)^t$ is used in our study. It reaches the best compromise between *noise* reduction and edge characterization.

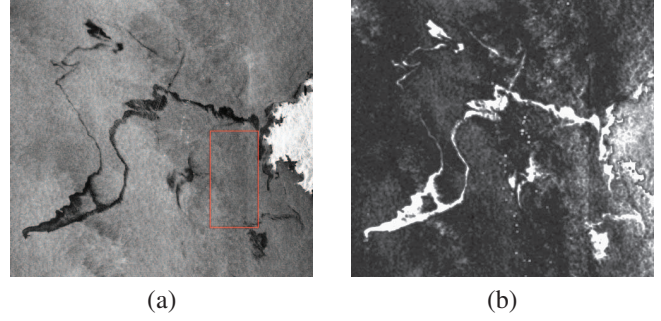


Fig. 2. (a) Envisat ASAR image to be processed. the rectangular area characterizes the ROI that defines normal sea state. (b) Similarity measure between local pdf (taken from a 15×15 sliding window) and pdf of normal sea surface.

2. The other strategy consists in using previous detection, yielded by eq. (4). This iterative pdf estimation reinforce the homogeneity in the neighbour of the central pixel.

In that case, the sliding window may be of increasing size or not.

Then, the initial set of pixels $\{x_1, x_2, \dots, x_n\}$, issued from the sliding window of central pixel x_{central} , is associated to a set $\{y_1, y_2, \dots, y_n\}$ of co-located criteria samples (the criteria at the central location is denoted y_{central}). For pdf estimation, each sample $x_i, i = 1, 2, \dots, n$ is taken into consideration if

$$t_{\text{inf}} \leq \frac{y_{\text{central}} - y_i}{y_{\text{central}}} \leq t_{\text{sup}} \quad (6)$$

where t_{inf} and t_{sup} are thresholds that adjust the selection level. y stands for a gradient measure when structural informations have to be taken into consideration. y stands for KL measure when an iterative process is used.

3. APPLICATION

When applied to Envisat ASAR image of Prestige tanker, 5 decompositions of the original image allows to smooth the texture and highlight the spills' borders. Fig. 2-(a) shows the ASAR image acquired on Nov. 17th, 2002, with the selected area considered as normal sea state. Fig. 2-(b) shows the preliminary result by considering local distribution contrast from the distribution of the normal sea area. This first result is a measure of similarity and no decision is taken at this level. It proves the consistency of this approach of slick detection purpose, with a better accuracy than direct thresholding technique.

In fact, this first result (by using a 15×15 sliding window) is a balance between good detection and false alarms reduction. Fig. 3 shows the benefits in using a gradient criteria in the characterization of the neighbourhood of the current

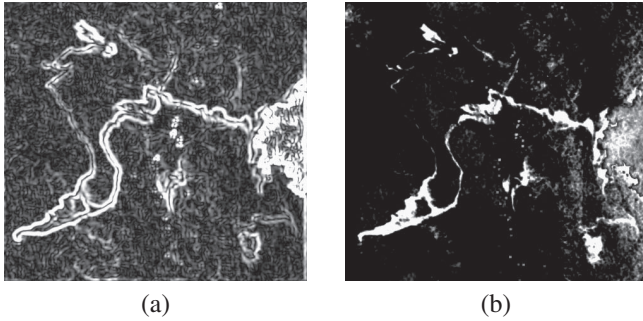


Fig. 3. Similarity measure for slick detection by considering criteria of eq. (6) in the selection of the samples in the neighbour of the current pixel. (a) Gradient magnitude image from eq. (5) with $L = 5$; (b) detection image.

pixel. It induces a significant reduction of the false alarms as it stands. Moreover, the detection of thin slicks remains accurate. Then, the result of fig. 3-(b) may be used as a criteria in eq. (6). Fig. 4 shows the detection results when the similarity measure is applied by considering the conditional results of previous detection. In that case, eq. (6) has been applied on the results of fig. 3-(b) with increasing window size. Results of fig. 3-(b) were obtained with a 9×9 sliding window whereas fig. 4 is based on a 15×15 window. Hence, the comparison from fig. 2-(b) proves the effectiveness of the overall strategy that keeps an accurate slick detection, even for small slick, while reducing false alarms.

When this strategy is applied to a range of window size, the final decision making can follow the use of similarity profiles as described in [2]. Fig. 5 shows typical examples of similarity profiles acquired on 4 areas corresponding to real slicks (thin or large but mixed up with clean water) and normal sea surface but of low radiometry. The similarity measures are of low level that may induce false alarms when a threshold

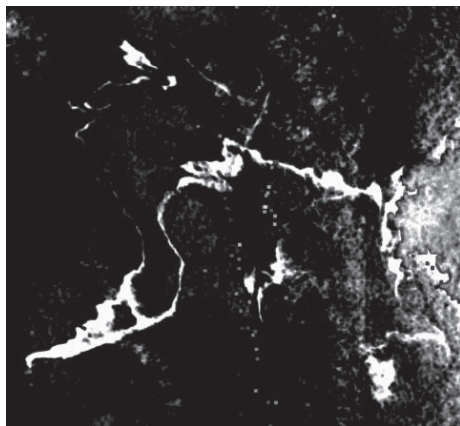


Fig. 4. Conditional detection by iteration of detection results.

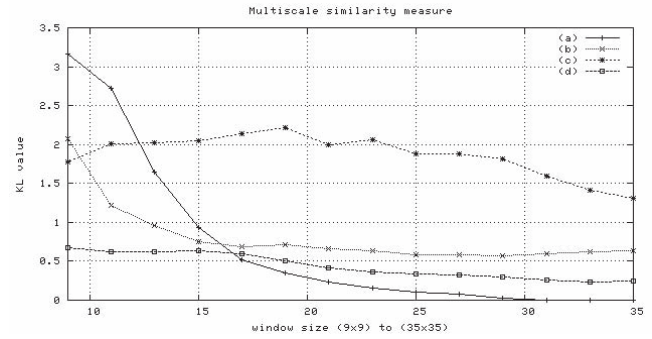


Fig. 5. Similarity profiles estimated with sliding windows of increasing size: from 9×9 to 35×35 . Profile (a) corresponds to measure in a fine slick, (b) to measure on a large degraded slick, (c) and (d) to measures in ambiguous areas.

is applied at each scale. Nevertheless, the shape of the profiles, over the size of estimation, induces specific signature than can be used for reducing false alarms. Signatures of ambiguous area tend to be of flat shape, whatever the level of the similarity value, while the signature involving real slicks is decreasing with the size of the window. This last observation will be used for our further developments.

References

- [1] European Space Agency (ESA), *Oil pollution monitoring in ERS and its applications: marine, the netherlands* : esa publications division edition, 1998, BR-128.
- [2] J Inglada and G Mercier, "A New Statistical Similarity Measure for Change Detection in Multitemporal SAR Images and its Extension to Multiscale Change Analysis," *IEEE Trans. Geosci. Remote Sensing*, vol. 45, no. 5, pp. 1432–1446, May 2007.
- [3] G Mercier and F Girard-Ardhuin, "Partially Supervised Oil Slick Detection by SAR Imagery using Kernel Expansion," *IEEE Trans. Geosci. Remote Sensing*, vol. 44, no. 10, pp. 2839–2846, Oct. 2006.
- [4] C L Nikias and A P Petropulu, *Higher-Order Spectra Analysis—a nonlinear signal processing framework*, Englewoods Cliff, NJ, PTR Prentice Hall, 1993.
- [5] A Stuart and J Keith Ord, *Kendall's advanced theory of Statistics*, Edward Arnold, 5th edition, 1991.
- [6] P McCullagh, *Tensor Methods in Statistics*, Chapman and Hall, London, 1987.
- [7] J Lin, N Saito, and R Levine, "Edgeworth approximation of the Kullback-Leibler distance towards problems in image analysis," Tech. Rep., University of California, Davis, 1999, <http://www.math.ucdavis.edu/~saito>.